Published in final edited form as:
Sci Transl Med. 2012 October 3; 4(154): 154ra134. doi:10.1126/scitranslmed.3003840.

Prevention of Alveolar Destruction and Airspace Enlargement in a Mouse Model of Pulmonary Lymphangioleiomyomatosis (LAM)

Elena A. Goncharova[1], **Dmitry A. Goncharov**[1], **Melane Fehrenbach**[1], **Irene Khavin**[1], **Blerina Ducka**[1], **Okio Hino**[2], **Thomas V. Colby**[3], **Mervyn J. Merrilees**[4], **Angela Haczku**[1], **Steven M. Albelda**[1,5], and **Vera P. Krymskaya**[1,*]

[1]Department of Medicine, University of Pennsylvania, Philadelphia, PA 19104, USA [2]Department of Pathology and Oncology, Juntendo University School of Medicine, Tokyo 170-8455, Japan [3]Department of Laboratory Medicine and Pathology, Mayo Clinic, Scottsdale, AZ 85259, USA [4]Department of Anatomy with Radiology, University of Auckland, Auckland 92019, New Zealand [5]Wistar Institute, Philadelphia, PA 19104, USA

Abstract

Pulmonary lymphangioleiomyomatosis (LAM) is a rare genetic disease characterized by neoplastic growth of atypical smooth muscle–like LAM cells, destruction of lung parenchyma, obstruction of lymphatics, and formation of lung cysts, leading to spontaneous pneumothoraces (lung rupture and collapse) and progressive loss of pulmonary function. The disease is caused by mutational inactivation of the tumor suppressor gene *tuberous sclerosis complex 1 (TSC1)* or *TSC2*. By injecting TSC2-null cells into nude mice, we have developed a mouse model of LAM that is characterized by multiple random TSC2-null lung lesions, vascular endothelial growth factor–D expression, lymphangiogenesis, destruction of lung parenchyma, and decreased survival, similar to human LAM. The mice show enlargement of alveolar airspaces that is associated with progressive growth of TSC2-null lesions in the lung, up-regulation of proinflammatory cytokines and matrix metalloproteinases (MMPs) that degrade extracellular matrix, and destruction of elastic fibers. TSC2-null lesions and alveolar destruction were differentially inhibited by the macrolide antibiotic rapamycin (which inhibits TSC2-null lesion growth by a cytostatic mechanism) and a 3-hydroxy-3-methylglutaryl coenzyme A reductase inhibitor, simvastatin (which inhibits growth of TSC2-null lesions by a predominantly proapoptotic mechanism). Treatment with simvastatin markedly inhibited MMP-2, MMP-3, and MMP-9 levels in lung and prevented alveolar destruction. The combination of rapamycin and simvastatin prevented both growth of TSC2-null lesions and lung destruction by inhibiting MMP-2, MMP-3, and MMP-9. Our findings demonstrate a mechanistic link between loss of TSC2 and alveolar destruction and suggest that treatment with rapamycin and simvastatin together could benefit patients with LAM by targeting cells with TSC2 dysfunction and preventing airspace enlargement.

*To whom correspondence should be addressed. krymskay@mail.med.upenn.edu.

SUPPLEMENTARY MATERIALS www.sciencetranslationalmedicine.org/cgi/content/full/4/154/154ra134/DC1

Author contributions: E.A.G., S.M.A., and V.P.K. designed the experiments. E.A.G., D.A.G., M.F., I.K., B.D., T.V.C., M.J.M., A.H., and V.P.K. performed the experiments and analyzed the data. O.H. provided original culture of TSC2-null cells. E.A.G., A.H., S.M.A., T.V.C., M.J.M., and V.P.K. wrote the paper.

Competing interests: The authors declare that they have no competing interests.

INTRODUCTION

Pulmonary lymphangioleiomyomatosis (LAM), a rare lung disease affecting predominantly women of childbearing age (1), is caused by mutational inactivation of the tumor suppressor gene *tuberous sclerosis complex 1 (TSC1)* or *TSC2*. LAM can be sporadic (LAM-S) or associated with hamartoma syndrome tuberous sclerosis (LAM-TS) and is characterized by neoplastic growth of smooth muscle (SM)–like LAM cells, destruction of lung parenchyma, formation of lung cysts, and obstruction of lung lymphatics. Patients exhibit shortness of breath, spontaneous pneumothoraces (lung rupture and collapse), and chylothorax (obstruction of the thoracic duct and leakage of lymphatic fluid into the pleural space) (1). *TSC1* mutations cause a less severe clinical phenotype than do *TSC2* mutations (2). In addition, about 40% of LAM-S and 80% of LAM-TS patients develop angiomyolipomas (AMLs)—benign tumors of SM, blood vessels, and fat cells in the kidney (1). It is not known how LAM cells deficient for TSC2 cause destruction of lung parenchyma or whether lung destruction in LAM can be ameliorated.

TSC1/TSC2 regulates mammalian target of rapamycin (mTOR), which forms two functionally distinct complexes: rapamycin-sensitive mTORC1 and rapamycin-insensitive mTORC2 (3). Rapamycin-insensitive regulation of the actin cytoskeleton occurs through mTORC2-dependent regulation of RhoA and Rac1 guanosine triphosphatases (GTPases) (3, 4), and Rac1 is required for mTOR activation (5). In TSC2-null and human LAM cells, Rho GTPase activity is required for cell adhesion, motility, proliferation, and survival (6–8). The invasive cell phenotype is associated with up-regulation of matrix metalloproteinases (MMPs), and loss of TSC2 causes up-regulation of MMPs (9–11).

The discovery that *TSC2* functions as a negative regulator of mTORC1 (3, 12–14) led to clinical trials that tested the effect of the rapamycin analog sirolimus on LAM disease (15, 16). At nanomolar concentrations, rapamycin forms a complex with the immunofilin FKBP12 that allosterically inhibits mTORC1 (3). In some patients with LAM, sirolimus slows disease progression (15). Cessation of therapy, however, is associated with regression of pulmonary function (15). Thus, there is a need for alternative therapies to treat pulmonary LAM that target LAM cell survival and the cystic airspace enlargement.

In a recent study, we used the combination of rapamycin and simvastatin to abrogate TSC2-null tumor recurrence in mice carrying TSC2-deficient xenographic flank tumors (8). Simvastatin, a 3-hydroxy-3-methylglutaryl coenzyme A reductase inhibitor that modulates lipid metabolism, shows pleiotropic effects including inhibition of Rho GTPases, prevention of cancer (17), and prevention of experimental emphysema (18). However, the generalizability of drug effects on the TSC2-null flank tumors is limited and is unlikely to predict responses of the LAM lung.

A major limitation in understanding the mechanism of lung destruction in LAM and in identifying new therapeutic strategies has been the lack of a good animal model (19). Homozygous $TSC1^{-/-}$ and $TSC2^{-/-}$ mice are embryonic lethals (19), and the major spontaneous tumors in heterozygous $TSC1^{+/-}$ and $TSC2^{+/-}$ mice are kidney cystadenomas and liver hemangiomas (19). The spontaneous occurrence of lung tumors without apparent destruction of lung parenchyma in heterozygous $TSC1^{+/-}$ and $TSC2^{+/-}$ mice and in Eker rats with naturally occurring *TSC2* mutations is extremely rare and only occurs late in the animals' life (19). Thus, an experimental mouse model with TSC2-null lesions that shows lung parenchymal changes would be useful to identify mechanisms of alveolar destruction in LAM and to develop therapeutic strategies to prevent these changes. Here, we report the development of a TSC2-null mouse LAM model that can be used to investigate the link

between *TSC2* loss and cystic destruction in LAM. We also characterize the effect of two drugs (rapamycin and simvastatin) on emphysematous lung destruction.

RESULTS

TSC2 loss induces lung lesions

Circulating LAM cells have been isolated from peripheral blood (20) and chylous effusions (21), suggesting that LAM cells may behave like metastatic tumor cells. However, the *TSC2*-related renal lesions such as AMLs, renal oncocytoma, and renal cell carcinoma (RCC) in human LAM (22) or cystadenoma and RCC in mice (19) are considered benign and cannot be classified as true RCC because they are not of renal epithelial origin (23).

To develop an animal model of LAM, we used TSC2-null cells derived from mouse kidney lesions that can spontaneously develop in heterozygous $TSC2^{+/-}$ mice (19, 24). Because these cells rarely formed lung lesions when directly injected into the tail vein of nude mice, we enhanced their neoplastic characteristics as follows (fig. S1). Cells from kidney lesions were injected into the flanks of athymic nude mice. The resulting tumors were dissociated, and cells were passaged. These TSC2-null tumor cells show mTORC1 activation, high proliferation rate without growth factor stimuli, migration, invasiveness, and SM α-actin expression similar to human LAM cells (Figs. 1, A and B, and 3A and fig. S2A) (7, 12, 25, 26). Injection of the TSC2-null tumor cells into the tail veins of nude mice induced growth of multiple lesions in the lung (Figs. 1, C and D, and 2 and figs. S3 and S4). No visible tumors were observed in kidney, spleen, liver, heart, intestine, or uterus.

TSC2-null lesions induce alveolar destruction and airspace enlargement in lungs

In pulmonary LAM, it is not known whether airspace enlargement occurs as a result of TSC2 loss in LAM cells. To address this question, we performed morphometric analysis of lungs from control mice and mice with TSC2-null lesions. To ensure that the lungs were processed under the same experimental conditions and to preserve the lung architecture, we inflated lungs from control and experimental animals at a constant 25-cm H_2O pressure, followed by fixation as described in Materials and Methods. Hematoxylin and eosin (H&E) staining of control lungs showed typical lung structure with conducting airways, branching bronchioles, and alveoli (Figs. 1D and 2 and fig. S3). Lungs with TSC2-null lesions showed multiple lesions surrounded by thin-walled alveoli with multiple enlarged airspaces (Figs. 1D and 2 and fig. S3). The TSC2-null lesions stained positive for SM α-actin, as is also seen in human LAM lungs, and for phospho-S6 (P-S6), the molecular signature of mTORC1 activation in LAM (12) (Fig. 3, B and C, respectively).

To determine that enlarged airspaces were induced specifically by loss of TSC2 in the lesions, we reexpressed TSC2 in TSC2-null cells to use as a control. Reexpression of TSC2 not only inhibited cell growth but also prevented the ability of these cells to form tumors. As an alternative approach, we used Lewis lung carcinoma (LLC) cells, an established model of mouse lung cancer (27). LLC cells expressed TSC2 (Fig. 1A), formed multiple lung lesions (Fig. 1D), and were negative for P-S6 and SM α-actin (Fig. 3, B and C). Lung parenchyma surrounding TSC2-expressing LLC lesions is comparable to that found in control animals (Fig. 1D). Morphometric analysis of H&E sections, assessed by measurement of the mean linear intercept (MLI) (a mean of chord lengths between intersections with alveoli) and mean alveolar airspace area (MAAA) (28) (the average area of alveoli in examined fields), showed a statistically significant increase in alveolar airspace in lungs with TSC2-null lesions compared to lungs with LLC lesions and control lungs (Fig. 1, E and F). As an additional control, we measured MLI and MAAA in mouse lungs bearing $TSC2^{+/+}p53^{-/-}$ lesions and found no alveolar space enlargement (Fig. 1, D to F). In immunocompetent

C57BL/6 mice, TSC2-null cells also formed lung lesions that induced alveolar space enlargement (Fig. 1, E and F). Increases in airspace enlargement dependent on the percentage of the TSC2-null lesion area to the total lung area indicate that progressive destruction of lung parenchyma is induced by growth of TSC2-null but not TSC2-expressing lesions (Fig. 2).

Comparison of lung morphology with human LAM shows that TSC2-null lesions in mice appear to contain more cells than human LAM lesions and that TSC2-null lesions in mice tend to accumulate around veins, arteries, or airways (fig. S4), a feature present but less prominent in human LAM lesions. Also, a predominant feature in human LAM is holes/cysts with modest increase in alveolar size (29), whereas in the mouse model, only enlargement of alveolar spaces was observed. TSC2-null lesions in mice show SM α-actin expression (Fig. 3B), a characteristic feature of human LAM (1). Furthermore, in both TSC2-null lesions in mice and in human LAM, a biomarker of TSC2 loss, mTORC1 activation, was detected by phosphorylation of ribosomal protein S6 (Fig. 3C). Collectively, these data demonstrate that although the mouse model may not be a perfect morphological model for human LAM, this model has proliferating SM α-actin-positive TSC2-null cells inducing progressive alveolar destruction in the lung.

TSC2-null lesions express vascular endothelial growth factor–D and promote lymphangiogenesis

Lymphatic involvement in human LAM has been demonstrated by abundant lymphatics in human LAM lungs and LAM lesions (30) and is associated with high levels of lymphatic growth factor vascular endothelial growth factor–D (VEGF-D) in the serum of subjects with LAM disease (31). Lungs from mice with TSC2-null lesions showed marked immunoreactivity for VEGF-D, similar to VEGF-D immunoreactivity in human LAM tissue samples as shown in Fig. 3D. Nodules from LAM patients have pronounced lymphatic channels lined by endothelial cells (30) (Fig. 3E). In the mouse model, numerous lymphatic vessels were detected in TSC2-null lesions with antibody for the hyaluronan receptor (*LYVE-1*), a marker of lymphatic vessels (Fig. 3E). These data demonstrate increased VEGF-D expression and lymphangiogenesis in the TSC2-null mouse model of LAM, which have also been observed in human LAM.

TSC2-null lung lesions induce MMP expression and elastin fiber degradation

The prevailing hypothesis for the mechanism of parenchymal destruction and cystic lung formation in LAM is that it is mediated by MMPs that particularly target elastin. In LAM, MMP-2—which acts on substrates including elastin and collagens I, III, and IV—is up-regulated in an mTORC1-independent manner without significant change in expression of tissue inhibitors of metalloproteinases (TIMPs) (9). Here, MMP-2 and MMP-3 (elastin and collagens III and IV) and MMP-9 (elastin and collagen IV), analyzed by enzyme-linked immunosorbent assay (ELISA), were significantly increased in bronchoalveolar lavage (BAL) fluid from mice with TSC2-null lesions compared with age-matched controls (Fig. 4, A to C) (32). Immunohistochemical analysis of lungs with TSC2-null lesions also showed significant increases in MMP-7 (elastin and collagens I, III, and IV), MMP-9, and MMP-12 (elastin and collagens I and IV) (fig. S5, A, C, and D). MMP-8 (collagens I and III) immunostaining was also increased in lungs with TSC2-null and TSC2-expressing lesions compared to control lungs (fig. S5B). These data demonstrate differential expression of MMPs in lungs with TSC2-null and TSC2-expressing lesions, in particular of those MMPs that target elastin and collagens of various types. Notably, these changes in MMP levels occurred in a time-dependent manner, consistent with increases in lesion growth and lung destruction (Fig. 2).

Because lung destruction in LAM is a result, at least in part, of elastic fiber degradation (33), we examined elastin and collagen composition using Verhoeff's elastin and Picro-Ponceau counterstaining (34). In normal mouse lungs, elastin (Fig. 4, D and F, black) and collagen (Fig. 4, D and F, red) fibers are especially concentrated around the rim or neck of each alveolus (arrows in Fig. 4D). The alveoli of animals with TSC2-null lesions exhibited a significant loss of elastin in the neck region as shown by a decrease in black staining and statistical analysis (Fig. 4, E to G). Morphometric analysis confirmed a statistically significant decrease in elastin but not collagen content in alveoli of mouse lungs with TSC2-null lesions (Fig. 4E). These data demonstrate that growth of TSC2-null lesions is preferentially associated with elastic fiber loss, consistent with the increase in MMPs known to target elastin (35).

Neoplastic lesion progression is also characterized by a time-dependent activation of innate immune-derived mediators. Although no LAM-specific cytokine/chemokine profile has been identified to date, human LAM has been associated with increased CXCL1 (KC), CCL2 (MCP1), and CXCL5 (36). These chemokines could be up-regulated by interleukin-1β (IL-1β), tumor necrosis factor–α (TNF-α), and/or IL-6. IL-1β and IL-6 are strongly associated with tumor growth, and TNF-α signaling is directly linked to the TSC1/TSC2-mTOR through nuclear factor κB (NF-κB)/inhibitor of NF-κB kinase β (IKKβ) (37). To investigate the inflammatory response to growth of TSC2-null lesions in the lung, we measured TNF-α, IL-1β, IL-6, and the chemokines KC/CXCL1 (the human IL-8 equivalent) and eotaxin/CCL11, the receptor of which (CCR3) occurs in primary LAM tissue (36). We noted modest, but significant, release of each of these proinflammatory mediators during lesion progression (Fig. 4, H to L). TNF-α, IL-1β, and KC expression peaked 2 weeks after inoculation of tumor cells and showed a decline by day 20. IL-6 and eotaxin levels continuously increased up to day 20. Consistent with the fact that the tumor recipient mice were nude mice, there was no T cell–derived cytokine [interferon-γ (IFN-γ) and IL-4] expression, with the exception of minimally elevated IL-13 levels. Immunostaining with the macrophage marker F4/80 showed influx of macrophages into TSC2-null lesions (fig. S6). The kinetics of the release of proinflammatory mediators (Fig. 4, H to L) coincided with the influx of inflammatory cells into the airways (Fig. 4M and fig. S6), suggesting that these mediators may drive a proinflammatory response during tumor cell invasion of the lung tissue.

Rapamycin plus simvastatin prevents TSC2-null lesion growth and lung parenchyma destruction

We assessed whether rapamycin or simvastatin, alone or in combination, could prevent tumor growth of TSC2-null lesions and alveolar destruction in our mouse model of LAM. Before in vivo experiments, background cell culture analysis was performed to determine growth-inhibitory effects of rapamycin and simvastatin on TSC2-null cells used to establish the LAM mouse model. Rapamycin or simvastatin alone markedly inhibited TSC2-null proliferation (fig. S2, B and C), but the combination of these two drugs induced greater inhibition of TSC2-null cell proliferation than either drug alone (fig. S2D). The rapamycin and simvastatin doses and treatment schedules were selected on the basis of our published data (8). The drug treatment started at day 3 after TSC2-null cells were injected into mice (Fig. 5A).

Animals treated with vehicle progressively lost weight after day 11 and were sacrificed at day 20 (Fig. 5A). Vehicle-treated animals developed multiple large lung lesions with increased alveolar spaces in the surrounding parenchyma (Fig. 5B). All mice were sacrificed at day 20. Mice treated with rapamycin and simvastatin alone or in combination did not lose weight compared to vehicle-treated mice (Fig. 5A) and were comparable in weight to control mice given the same treatment (Fig. 5A). Rapamycin alone and in combination with

simvastatin prevented TSC2-null lesion growth (Fig. 5, B and C). Simvastatin alone decreased the amount of lesion/lung compared to vehicle-treated mice (Fig. 5, B and C). Treatments with rapamycin, simvastatin, or both also prevented alveolar space enlargement (Fig. 5D).

Both rapamycin and simvastatin significantly decreased MMP-2 levels in BAL (Fig. 5E), whereas MMP-3 and MMP-9 expression was markedly and significantly reduced in simvastatin- but not rapamycin-treated animals (Fig. 5, F and G), demonstrating that rapamycin and simvastatin have differential inhibitory effects on MMP-3 and MMP-9. The combined treatment abrogated the increases in both MMP-3 and MMP-9 (Fig. 5, F and G).

Rapamycin and simvastatin treat established TSC2-null lesions and lung parenchyma destruction

To determine whether rapamycin and simvastatin could inhibit the growth of well-developed TSC2-null lesions, we treated TSC2-null lung lesion–bearing mice at day 10, a time when mice have begun to develop TSC2-null lung lesions and show destruction of lung parenchyma, but before the changes are statistically significant (Fig. 2B). Treatment with each drug alone on day 10 reduced TSC2-null cell proliferation as detected by immunostaining with Ki67 (Fig. 6A and fig. S7A) and by a decreased proportion of the lung occupied by lesion (Fig. 6D). As we showed previously (8), rapamycin but not simvastatin inhibited mTORC1-dependent S6 phosphorylation in TSC2-null lesions (Fig. 6B and fig. S7B), but rapamycin did not promote apoptosis, whereas simvastatin did (Fig. 6C and fig. S7C). Simvastatin alone inhibited lesion growth (Fig. 6A and fig. S7A) and induced apoptosis (Fig. 6C and fig. S7C) but had little effect on P-S6 levels (Fig. 6B and fig. S7B). Rapamycin and simvastatin combined showed modest effect on DNA synthesis and cell apoptosis in TSC2-null lesions (Fig. 6, A and C, and fig. S7, A and C).

Nevertheless, morphometric analyses of lung tissue sections treated under the same experimental conditions showed a significant decrease in alveolar space enlargement in animals treated with simvastatin alone (Fig. 6, E and F). Rapamycin alone did not significantly decrease MLI and MAAA compared to untreated animals (Fig. 6, E and F) and only modestly improved the beneficial effect of simvastatin on preventing an alveolar space enlargement (Fig. 6, E and F). The simvastatin-induced reduction in alveolar destruction occurred when the lesion sizes were equivalent to those of the rapamycin-treated mice (Fig. 6D). These data demonstrate that, whereas rapamycin and simvastatin can each inhibit TSC2-null lesion growth, simvastatin prevents alveolar destruction.

DISCUSSION

We have demonstrated that our mouse model of LAM carries TSC2-null lesions that showed SM α-actin expression, mTORC1 activation, VEGF-D expression, and increased lymphangiogenesis, as well as destruction of lung parenchyma, all of which are characteristics of human pulmonary LAM. Our data showed that progressive growth of TSC2-null lung lesions induced MMP up-regulation and elastin fiber degradation in the lung. These findings suggest that the cystic lung destruction seen in LAM is associated with loss of TSC2. We also have shown that rapamycin inhibits lesion growth, simvastatin prevents alveolar space enlargement, and treatment with a combination of rapamycin and simvastatin abolishes MMP up-regulation and TSC2-null lesion growth and prevents alveolar destruction. The results reported here thus support further investigation of the combination of rapamycin and simvastatin as a potential treatment for subjects with LAM. It is possible that other diseases associated with TSC2 deficiency could benefit from the same combinational treatment strategy. Abnormal enlargement of airspaces is a major pathological manifestation of many lung diseases including emphysema, chronic obstructive

pulmonary disease (COPD), cystic fibrosis, pulmonary LAM, and Birt-Hogg-Dube syndrome. Although the etiologies of these diseases are different, alveolar destruction is a common pathobiological manifestation associated with cystic airspace enlargement.

The prevailing hypothesis is that lung destruction and cystic space formation in patients with LAM are mediated by degradation of extracellular matrix as a result of an imbalance between matrix-degrading proteases (MMPs) and their endogenous inhibitors TIMPs (38). Indeed, elastic fibers in remodeled alveoli in lungs from LAM patients are scant, and those that remain are often disrupted (33). Similarly, in our study, significant decreases in elastin fibers were seen in alveoli of mice bearing TSC2-null lesions. Increased MMP-1, MMP-2, MMP-9, MMP-11, and MMP-19 levels have been reported in lungs from patients with LAM (39), and mTORC1-independent up-regulation of MMP-2 expression was shown in TSC2-deficient cells and cells from LAM patients (9–11). Our data demonstrate that growth of TSC2-null lesions in murine lung is associated with an increase in MMP-2, MMP-3, MMP-7, MMP-9, and MMP-12 levels, all with known elastase activity (35). Note that these MMPs also target collagens, including type I, but when examined histologically, collagen content was not significantly decreased where it is most concentrated, in the alveolar rims. The extent to which altered amounts of TIMPs are involved in alveolar destruction in this model remains to be determined.

The increase in proinflammatory cytokines in the LAM model suggests that inflammation may also contribute to the destruction of alveoli, given cytokine stimulation of MMPs (35). This process could provide an amplifying feedback loop in the alveolar destruction pathway. Further studies are needed in the TSC2-null mouse model of LAM to determine the relative contribution of TSC2-null lesions in increased expression of MMPs and the recruitment of inflammatory cells and cytokines to alveolar destruction in LAM. These would probably be most informative in further studies in immunocompetent mice where TSC2-null lesions also induce alveolar space enlargement.

Pulmonary LAM is accompanied by increased lymphangiogenesis in the lung and LAM nodules (40) and increased concentrations of VEGF-D, a lymphangiogenic growth factor (41) that has been found in the serum of subjects with LAM (31). The increased VEGF-D and increased number of lymphatic vessels in TSC2-null lesions in our mice echo these features.

We acknowledge that the model is not a perfect replica of human LAM, but it is similar in many ways—notably, progressive growth of SM α-actin–positive TSC2-null lesions, destruction of lung parenchyma, and lymphatic involvement. In human disease, rounded cystic change is usually more pronounced and more widespread and, in some cases, associated with relatively few LAM cells (typically as scattered fascicles in the cyst walls) compared to our mouse model in which the destruction of alveoli and airspace enlargement usually directly surrounds TSC2-null lesions and large rounded cysts are not a feature. In addition, the mouse lesions contain more TSC-null cells than most human lesions, and the cells showed some tendency to accumulate in perivascular regions of both arteries and veins, a feature not prominent in human LAM but one that can be encountered and is seen in metastases of a variety of tumors to the lungs in humans (29). This relatively localized damage in mice could result from the exponential growth of the TSC2-null cells in a short period of time [about 3 weeks from injection to sacrifice, in compliance with Institutional Animal Care and Use Committee (IACUC) protocol] in the immunocompromised mice. The use of immunocompetent mice and injection of fewer TSC2-null cells might produce more diffuse airspace destruction, producing pathology closer to that of human LAM.

With these caveats in mind, we used our model to test the potential use of both rapamycin and simvastatin for combination therapy in pulmonary LAM. Despite promising results of rapamycin analog sirolimus in the clinic for LAM (15), after cessation of sirolimus therapy, pulmonary function reverts to the diminished levels observed before treatment (15), likely because sirolimus does not completely inhibit mTORC1 signaling, but only inhibits LAM cell growth without promoting cell death (8). Further, an undesirable side effect, hyperlipidemia, occurs in LAM and TS patients on sirolimus (15, 42).

Statins, well known as cholesterol-lowering drugs, also inhibit experimental emphysema (43) and MMP-9 secretion (44) and have anti-inflammatory effects in a variety of diseases such as COPD (18), cancer (45), and asthma (46). These drugs modulate lipid metabolism and disrupt the geranylgeranylation of Rho GTPases that is critical for membrane localization and activation. The safety and efficacy of statins as cholesterol-lowering drugs are well documented and indicate that simvastatin and atorvastatin are the most potent agents. Atorvastatin inhibited growth of $TSC2^{-/-}p53^{-/-}$ mouse embryonic fibroblasts (MEFs) and TSC2-null ELT3 cells from Eker rat in vitro (47) but had little effect on subcutaneous tumors formed by $TSC2^{-/-}p53^{-/-}$ MEFs (48). In previous studies on mice with subcutaneous tumors formed by TSC2-null ELT3 cells, we showed that loss of TSC2 activates the rapamycin-sensitive mTORC1-S6K1 (S6 kinase 1) and the rapamycin-resistant mTORC2–Rho GTPase signaling pathways (fig. S8A) [the latter is inhibited by the nonselective Rho GTPase inhibitor simvastatin (8)]. Here, treatment with rapamycin and simvastatin also prevented TSC2-null lesion development. However, in the mouse LAM model, we also saw prevention of alveolar airspace enlargement and decreased MMP expression, suggesting that the destruction of lung parenchyma is caused by TSC2-null lesion growth (fig. S8B). The doses and treatment schedule for rapamycin were selected on the basis of the pharmaco-kinetics and pharmacodynamics approved for immunosuppression after organ transplantation, clinical trials, and rodent studies (8, 15, 18). Although a relatively high dose of simvastatin was used in this study, because mice metabolize simvastatin more rapidly than humans, lower doses may be effective in humans. A retrospective study of LAM patients on statins cautioned about potential effects of statins on lung function, without taking into account intermolecular differences between statins (49). Thus, a comparison of different statins in preclinical studies on the same cell and animal models is still needed, and their pharmacological characteristics and safety in LAM remain to be determined.

Our data show that rapamycin and simvastatin have differential effects on TSC2-null lesion growth and alveolar space enlargement. (See schematic representation of TSC2-dependent signaling in LAM and its potential therapeutic targeting in fig. S8.) Rapamycin had a predominantly growth-inhibitory effect on TSC2-null lesions, whereas simvastatin inhibited alveolar airspace enlargement, suggesting that the therapeutic approach currently being used for treatment of LAM (rapamycin) may not address the TSC2-dependent pathological changes of lung destruction. Our study predicts that rapamycin alone would not be effective in preventing MMP increases and lung destruction. However, further investigation will reveal whether rapamycin or simvastatin has specific inhibitory effects on MMPs or whether other factors induce airspace enlargement in this mouse model.

In summary, this study reports an experimental model for testing treatment strategies in pulmonary LAM and provides preclinical evidence of a proof of concept that pharmacological use of rapamycin and simvastatin is a promising strategy for LAM. Both rapamycin and simvastatin are in clinical use for other indications. A phase 2 clinical trial could test whether rapamycin and simvastatin in combination has beneficial effects on LAM.

MATERIALS AND METHODS

Cell culture

TSC2-null cells, derived from kidney lesions of *TSC2*$^{+/-}$ mice (24), mouse LLC, and mouse epithelial NMuMG cells, purchased from the American Type Culture Collection, and *Tsc2*$^{+/+}$*p53*$^{-/-}$ MEFs (provided by D. J. Kwiatkowski) were maintained in Dulbecco's modified Eagle's medium (DMEM) with 10% fetal bovine serum (FBS).

DNA synthesis analysis, cell counts, SM α-actin FACS analysis, and wound closure assay

These were performed as described (8, 12, 26, 50).

The human LAM and control lung tissue

Samples presented in Fig. 3 were obtained from the National Disease Research Interchange (NDRI) according to the approved protocol. The human LAM tissue presented in fig. S4 was obtained from the National Institutes of Health under the protocol approved by the National Heart, Lung, and Blood Institute and examined in compliance with the protocol approved by the University of Auckland Institutional Review Board (Auckland Ethics Committee, North Heath, New Zealand).

Animals

All animal procedures were performed according to a protocol approved by the University of Pennsylvania IACUC. Six- to 8-week-old female NCr athymic nu/nu mice (NCRNU-M, Taconic) were injected subcutaneously in both flanks with 5×10^6 TSC2-null mouse kidney epithelial cells (24) (fig. S1). When tumors reached ~1.5 cm in diameter, mice were sacrificed, and the tumors were removed, enzymatically digested, and plated in cell culture dishes in DMEM supplemented with 10% FBS. After 2 days in culture, the TSC2-null cells from the primary tumors were resuspended and filtered, and 10^6 cells were injected into the tail vein of 8-week-old NCRNU-M athymic nude mice. Three or 10 days after injection, mice were transferred to simvastatin-supplemented diet (100 mg/kg per day) or treated with rapamycin (intraperitoneal injections, 1 mg/kg, three times per week) alone or in combination with simvastatin diet. Chow containing simvastatin (ZOCOR, Merck) was prepared by Animal Specialties & Provision on the basis of regular chow JL Rat & Mouse/4F diet received by the control group. Negative controls included vehicle-injected mice treated as described above. For positive controls, the tail veins of NCRNU-M mice were injected with 10^6 LLC cells or *Tsc2*$^{+/+}$*p53*$^{-/-}$ MEFs that were rederived from subcutaneous tumors as described above for TSC2-null cells. Animal weight was monitored throughout the experiment. Animals injected with TSC2-null cells from each group were euthanized at day 0, 10, 12, 15, or 20 of the experiment. Control-, LLC-, and *Tsc2*$^{+/+}$*p53*$^{-/-}$ MEF–injected mice were euthanized at day 20 after injection or at 20% of body weight loss in the positive control group (TSC2-null vehicle). Lungs were inflated at 25-cm H_2O pressure with 1:1 optimal cutting temperature (OCT) in phosphate-buffered saline for ~8 min or in formalin. The trachea was tied off, and the lungs were excised, placed in OCT, flash-frozen on dry ice, and sectioned into 5-μm-thick slices followed by H&E staining and immunohistochemical analysis. Each experimental group included a minimum of five animals per condition. The tissue samples were analyzed by three different investigators at the University of Pennsylvania and by one investigator in New Zealand. Experiments to determine that TSC2-null lesions induce alveoli space enlargement were performed twice, and experiments with treatment by rapamycin, simvastatin, and the combination of both were performed three times.

Morphometry

Images of lung tissue sections stained with H&E were acquired with a Nikon Eclipse 80i microscope under ×100 magnification. Ten randomly selected fields per slide from three nonserial sections about 50 μm apart were captured, and Image-Pro Plus 6.2 software (Media Cybernetics Inc.) was used to measure the MAAA as described (28). Airspace changes were also assessed with the MLI, a measurement of mean interalveolar septal wall distance, which is widely used to examine irregular size alveoli. The MLI was measured by dividing the length of a line drawn across the lung section by the total number of intercepts counted within this line at ×100 magnification. A total of 40 lines per slide were drawn and measured. Airway, vascular structures, and histological mechanical artifacts were eliminated from the analysis.

The volume fraction (%) of elastic fibers was determined on images of tissue sections stained with Verhoeff's elastin stain and Picro-Ponceau counterstain with a 100-point grid to record hits over elastin and total tissue hits to give percentage of area occupied by elastin, as described (34).

BAL fluid was collected from five mice per each condition at days 0, 10, 12, 15, and 20 after injection of TSC2-null cells. BAL cell counts were assessed as described (32).

ELISA was performed with a Searchlight Protein Array multiplex of cell-free supernatant of the BAL fluids at Aushon Biosystems.

Immunohistochemical and immunoblot analyses

These were performed as described (6, 8). Immunostaining was analyzed with the Nikon Eclipse TE2000-E microscope equipped with an Evolution QEi digital video camera. Tumors from a minimum of five animals per each treatment condition were analyzed. Staining was visualized with a Nikon Eclipse TE2000-E microscope under appropriate filters. Protein levels were analyzed by OD with Gel-Pro Analyzer software.

Data analysis

Data points from individual assays represent means ± SE. Statistically significant differences among groups were assessed with ANOVA (with the Bonferroni-Dunn correction), with values of $P < 0.05$ sufficient to reject the null hypothesis for all analyses. All experiments were designed with matched control conditions within each experiment (minimum of five animals) to enable statistical comparison as paired samples and to obtain statistically significant data.

Supplementary Material

Refer to Web version on PubMed Central for supplementary material.

Acknowledgments

We thank D. J. Kwiatkowski (Brigham and Women's Hospital, Boston, MA) for $Tsc2^{+/+}p53^{-/-}$ MEFs, H. DeLisser (University of Pennsylvania) for LYVE-1 antibodies, S. Lu for help with cell growth experiments, and the NDRI for providing us with LAM tissue.

Funding: Supported by 2RO1HL71106 (V.P.K.), RO1HL090829 (V.P.K.), RO1HL114085 (V.P.K.), Abramson Cancer Center Core Support Grant NIH P130-CA-016520-34 (V.P.K.), P30ES013508 (V.P.K. and A.H.), RO1AI072197 (A.H.), and RC1ES018505 (A.H.) from the NIH; American Lung Association (ALA) CI-9813-N (V.P.K.); LAM Foundation (V.P.K.); and Auckland Medical Research Foundation Grant 1109001 (M.J.M.).

REFERENCES AND NOTES

1. Juvet SC, McCormack FX, Kwiatkowski DJ, Downey GP. Molecular pathogenesis of lymphangioleiomyomatosis: Lessons learned from orphans. Am. J. Respir. Cell Mol. Biol. 2007; 36:398–408. [PubMed: 17099139]
2. Dabora SL, Jozwiak S, Franz DN, Roberts PS, Nieto A, Chung J, Choy YS, Reeve MP, Thiele E, Egelhoff JC, Karprzyk-Obara J, Domanska-Pakiela D, Kwiatkowski DJ. Mutational analysis in a cohort of 224 tuberous sclerosis patients indicates increased severity of *TSC2*, compared with *TSC1*, disease in multiple organs. Am. J. Hum. Genet. 2001; 68:64–80. [PubMed: 11112665]
3. Zoncu R, Efeyan A, Sabatini DM. mTOR: From growth signal integration to cancer, diabetes and ageing. Nat. Rev. Mol. Cell Biol. 2011; 12:21–35. [PubMed: 21157483]
4. Jacinto E, Loewith R, Schmidt A, Lin S, Ruegg MA, Hall A, Hall MN. Mammalian TOR complex 2 controls the actin cytoskeleton and is rapamycin insensitive. Nat. Cell Biol. 2004; 6:1122–1128. [PubMed: 15467718]
5. Saci A, Cantley LC, Carpenter CL. Rac1 regulates the activity of mTORC1 and mTORC2 and controls cellular size. Mol. Cell. 2011; 42:50–61. [PubMed: 21474067]
6. Goncharova E, Goncharov D, Noonan D, Krymskaya VP. TSC2 modulates actin cytoskeleton and focal adhesion through TSC1-binding domain and the Rac1 GTPase. J. Cell Biol. 2004; 167:1171–1182. [PubMed: 15611338]
7. Goncharova EA, Goncharov DA, Lim PN, Noonan D, Krymskaya VP. Modulation of cell migration and invasiveness by tumor suppressor TSC2 in lymphangioleiomyomatosis. Am. J. Respir. Cell Mol. Biol. 2006; 34:473–480. [PubMed: 16388022]
8. Goncharova EA, Goncharov DA, Li H, Pimtong W, Lu S, Khavin I, Krymskaya VP. mTORC2 is required for proliferation and survival of TSC2-null cells. Mol. Cell. Biol. 2011; 31:2484–2498. [PubMed: 21482669]
9. Lee PS, Tsang SW, Moses MA, Trayes-Gibson Z, Hsiao LL, Jensen R, Squillace R, Kwiatkowski DJ. Rapamycin-insensitive up-regulation of *MMP2* and other genes in tuberous sclerosis complex 2-deficient lymphangioleiomyomatosis-like cells. Am. J. Respir. Cell Mol. Biol. 2010; 42:227–234. [PubMed: 19395678]
10. Chang WYC, Clements D, Johnson SR. Effect of doxycycline on proliferation, MMP production, and adhesion in LAM-related cells. Am. J. Physiol. Lung Cell. Mol. Physiol. 2010; 299:L393–L400. [PubMed: 20581100]
11. Moir LM, Ng HY, Poniris MH, Santa T, Burgess JK, Oliver BGG, Krymskaya VP, Black JL. Doxycycline inhibits matrix metalloproteinase-2 secretion from TSC2-null mouse embryonic fibroblasts and lymphangioleiomyomatosis cells. Br. J. Pharmacol. 2011; 164:83–92. [PubMed: 21418186]
12. Goncharova EA, Goncharov DA, Eszterhas A, Hunter DS, Glassberg MK, Yeung RS, Walker CL, Noonan D, Kwiatkowski DJ, Chou MM, Panettieri RA Jr. Krymskaya VP. Tuberin regulates p70 S6 kinase activation and ribosomal protein S6 phosphorylation. A role for the *TSC2* tumor suppressor gene in pulmonary lymphangioleiomyomatosis (LAM). J. Biol. Chem. 2002; 277:30958–30967. [PubMed: 12045200]
13. Krymskaya VP, Goncharova EA. PI3K/mTORC1 activation in hamartoma syndromes: Therapeutic prospects. Cell Cycle. 2009; 8:403–413. [PubMed: 19177005]
14. Marygold SJ, Leevers SJ. Growth signaling: TSC takes its place. Curr. Biol. 2002; 12:R785–R787. [PubMed: 12445406]
15. McCormack FX, Inoue Y, Moss J, Singer LG, Strange C, Nakata K, Barker AF, Chapman JT, Brantly ML, Stocks JM, Brown KK, Lynch JP III, Goldberg HJ, Young LR, Kinder BW, Downey GP, Sullivan EJ, Colby TV, McKay RT, Cohen MM, Korbee L, Taveira-DaSilva AM, Lee HS, Krischer JP, Trapnell BC. National Institutes of Health Rare Lung Diseases Consortium; MILES Trial Group, Efficacy and safety of sirolimus in lymphangioleiomyomatosis. N. Engl. J. Med. 2011; 364:1595–1606. [PubMed: 21410393]
16. Krymskaya VP. Treatment option(s) for pulmonary lymphangioleiomyomatosis: Progress and current challenges. Am. J. Respir. Cell Mol. Biol. 2012; 46:563–565. [PubMed: 22550272]

17. Demierre MF, Higgins PDR, Gruber SB, Hawk E, Lippman SM. Statins and cancer prevention. Nat. Rev. Cancer. 2005; 5:930–942. [PubMed: 16341084]
18. Barnes PJ. Future treatments for chronic obstructive pulmonary disease and its comorbidities. Proc. Am. Thorac. Soc. 2008; 5:857–864. [PubMed: 19017741]
19. Kwiatkowski DJ. Animal models of lymphangioleiomyomatosis (LAM) and tuberous sclerosis complex (TSC). Lymphat. Res. Biol. 2010; 8:51–57. [PubMed: 20235887]
20. Crooks DM, Pacheco-Rodriguez G, DeCastro RM, McCoy JP Jr. Wang JA, Kumaki F, Darling T, Moss J. Molecular and genetic analysis of disseminated neoplastic cells in lymphangioleiomyomatosis. Proc. Natl. Acad. Sci. U.S.A. 2004; 101:17462–17467. [PubMed: 15583138]
21. Kumasaka T, Seyama K, Mitani K, Souma S, Kashiwagi S, Hebisawa A, Sato T, Kubo H, Gomi K, Shibuya K, Fukuchi Y, Suda K. Lymphangiogenesis-mediated shedding of LAM cell clusters as a mechanism for dissemination in lymphangioleiomyomatosis. Am. J. Surg. Pathol. 2005; 29:1356–1366. [PubMed: 16160479]
22. Franz DN, Bissler JJ, McCormack FX. Tuberous sclerosis complex: Neurological, renal and pulmonary manifestations. Neuropediatrics. 2010; 41:199–208. [PubMed: 21210335]
23. Pavlovich CP, Schmidt LS. Searching for the hereditary causes of renal-cell carcinoma. Nat. Rev. Cancer. 2004; 4:381–393. [PubMed: 15122209]
24. Kobayashi T, Minowa O, Kuno J, Mitani H, Hino O, Noda T. Renal carcinogenesis, hepatic hemangiomatosis, and embryonic lethality caused by a germ-line *Tsc2* mutation in mice. Cancer Res. 1999; 59:1206–1211. [PubMed: 10096549]
25. Goncharova EA, Goncharov DA, Spaits M, Noonan DJ, Talovskaya E, Eszterhas A, Krymskaya VP. Abnormal growth of smooth muscle–like cells in lymphangioleiomyomatosis: Role for tumor suppressor TSC2. Am. J. Respir. Cell Mol. Biol. 2006; 34:561–572. [PubMed: 16424383]
26. Goncharova EA, Lim P, Goncharov DA, Eszterhas A, Panettieri RA Jr. Krymskaya VP. Assays for in vitro monitoring of proliferation of human airway smooth muscle (ASM) and human pulmonary arterial vascular smooth muscle (VSM) cells. Nat. Protoc. 2006; 1:2905–2908. [PubMed: 17406550]
27. Hiratsuka S, Nakamura K, Iwai S, Murakami M, Itoh T, Kijima H, Shipley JM, Senior RM, Shibuya M. MMP9 induction by vascular endothelial growth factor receptor-1 is involved in lung-specific metastasis. Cancer Cell. 2002; 2:289–300. [PubMed: 12398893]
28. Hsia CC, Hyde DM, Ochs M, Weibel ER. ATS/ERS Joint Task Force on Quantitative Assessment of Lung Structure, An official research policy statement of the American Thoracic Society/ European Respiratory Society: Standards for quantitative assessment of lung structure. Am. J. Respir. Crit. Care Med. 2010; 181:394–418. [PubMed: 20130146]
29. Travis, WD.; Colby, TV.; Koss, MN.; Rosado-De-Christenson, ML.; Müller, NL.; King, TE, Jr.. AFIP Atlas of Nontumor Pathology: Non-Neoplastic Disorders of the Lower Respiratory Tract. American Registry of Pathology; Washington, DC: 2002. p. 147-159.
30. Kumasaka T, Seyama K, Mitani K, Sato T, Souma S, Kondo T, Hayashi S, Minami M, Uekusa T, Fukuchi Y, Suda K. Lymphangiogenesis in lymphangioleiomyomatosis: Its implication in the progression of lymphangioleiomyomatosis. Am. J. Surg. Pathol. 2004; 28:1007–1016. [PubMed: 15252306]
31. Young LR, Inoue Y, McCormack FX. Diagnostic potential of serum VEGF-D for lymphangioleiomyomatosis. N. Engl. J. Med. 2008; 358:199–200. [PubMed: 18184970]
32. Hortobágyi L, Kierstein S, Krytska K, Zhu X, Das AM, Poulain F, Haczku A. Surfactant protein D inhibits TNF-α production by macrophages and dendritic cells in mice. J. Allergy Clin. Immunol. 2008; 122:521–528. [PubMed: 18554706]
33. Fukuda Y, Kawamoto M, Yamamoto A, Ishizaki M, Basset F, Masugi Y. Role of elastic fiber degradation in emphysema-like lesions of pulmonary lymphangiomyomatosis. Hum. Pathol. 1990; 21:1252–1261. [PubMed: 2249838]
34. Merrilees MJ, Hankin EJ, Black JL, Beamont B. Matrix proteoglycans and remodelling of interstitial lung tissue in lymphangioleiomyomatosis. J. Pathol. 2004; 203:653–660. [PubMed: 15141380]

35. Sternlicht MD, Werb Z. How matrix metalloproteinases regulate cell behavior. Annu. Rev. Cell Dev. Biol. 2001; 17:463–516. [PubMed: 11687497]
36. Pacheco-Rodriguez G, Kumaki F, Steagall WK, Zhang Y, Ikeda Y, Lin JP, Billings EM, Moss J. Chemokine-enhanced chemotaxis of lymphangioleiomyomatosis cells with mutations in the tumor suppressor *TSC2* gene. J. Immunol. 2009; 182:1270–1277. [PubMed: 19155472]
37. Lee DF, Kuo HP, Chen CT, Hsu JM, Chou CK, Wei Y, Sun HL, Li LY, Ping B, Huang WC, He X, Hung JY, Lai CC, Ding Q, Su JL, Yang JY, Sahin AA, Hortobagyi GN, Tsai FJ, Tsai CH, Hung MC. IKKβ suppression of TSC1 links inflammation and tumor angiogenesis via the mTOR pathway. Cell. 2007; 130:440–455. [PubMed: 17693255]
38. Krymskaya VP, Shipley JM. Lymphangioleiomyomatosis: A complex tale of serum response factor–mediated tissue inhibitor of metalloproteinase-3 regulation. Am. J. Respir. Cell Mol. Biol. 2003; 28:546–550. [PubMed: 12707009]
39. Hayashi T, Fleming MV, Stetler-Stevenson WG, Liotta LA, Moss J, Ferrans VJ, Travis WD. Immunohistochemical study of matrix metalloproteinases (MMPs) and their tissue inhibitors (TIMPs) in pulmonary lymphangioleiomyomatosis (LAM). Hum. Pathol. 1997; 28:1071–1078. [PubMed: 9308732]
40. Glasgow CG, Avila NA, Lin JP, Stylianou MP, Moss J. Serum vascular endothelial growth factor-D levels in patients with lymphangioleiomyomatosis reflect lymphatic involvement. Chest. 2009; 135:1293–1300. [PubMed: 19420197]
41. Seyama K, Mitani K, Kumasaka T, Gupta SK, Oommen S, Liu G, Ryu JH, Vlahakis NE. Lymphangioleiomyoma cells and lymphatic endothelial cells: Expression of VEGFR-3 in lymphangioleiomyoma cell clusters. Am. J. Pathol. 2010; 176:2051–2052. [PubMed: 20203284]
42. Dabora SL, Franz DN, Ashwal S, Sagalowsky A, DiMario FJ Jr. Miles D, Cutler D, Krueger D, Uppot RN, Rabenou R, Camposano S, Paolini J, Fennessy F, Lee N, Woodrum C, Manola J, Garber J, Thiele EA. Multicenter phase 2 trial of sirolimus for tuberous sclerosis: Kidney angiomyolipomas and other tumors regress and VEGF-D levels decrease. PLoS One. 2011; 6:e23379. [PubMed: 21915260]
43. Takahashi S, Nakamura H, Seki M, Shiraishi Y, Yamamoto M, Furuuchi M, Nakajima T, Tsujimura S, Shirahata T, Nakamura M, Minematsu N, Yamasaki M, Tateno H, Ishizaka A. Reversal of elastase-induced pulmonary emphysema and promotion of alveolar epithelial cell proliferation by simvastatin in mice. Am. J. Physiol. Lung Cell. Mol. Physiol. 2008; 294:L882–L890. [PubMed: 18310229]
44. Bellosta S, Via D, Canavesi M, Pfister P, Fumagalli R, Paoletti R, Bernini F. HMG-CoA reductase inhibitors reduce MMP-9 secretion by macrophages. Arterioscler. Thromb. Vasc. Biol. 1998; 18:1671–1678. [PubMed: 9812903]
45. Jain MK, Ridker PM. Anti-inflammatory effects of statins: Clinical evidence and basic mechanisms. Nat. Rev. Drug Discov. 2005; 4:977–987. [PubMed: 16341063]
46. Camoretti-Mercado B. Targeting the airway smooth muscle for asthma treatment. Transl. Res. 2009; 154:165–174. [PubMed: 19766960]
47. Finlay GA, Malhowski AJ, Liu Y, Fanburg BL, Kwiatkowski DJ, Toksoz D. Selective inhibition of growth of *tuberous sclerosis complex 2*–null cells by atorvastatin is associated with impaired Rheb and Rho GTPase function and reduced mTOR/S6 kinase activity. Cancer Res. 2007; 67:9878–9886. [PubMed: 17942919]
48. Lee N, Woodrum CL, Nobil AM, Rauktys AE, Messina MP, Dabora SL. Rapamycin weekly maintenance dosing and the potential efficacy of combination sorafenib plus rapamycin but not atorvastatin or doxycycline in tuberous sclerosis preclinical models. BMC Pharmacol. 2009; 9:8. [PubMed: 19368729]
49. El-Chemaly S, Taveira-DaSilva A, Stylianou MP, Moss J. Statins in lymphangioleiomyomatosis: A word of caution. Eur. Respir. J. 2009; 34:513–514. [PubMed: 19648526]
50. Shang Y, Yoshida T, Amendt BA, Martin JF, Owens GK. Pitx2 is functionally important in the early stages of vascular smooth muscle cell differentiation. J. Cell Biol. 2008; 181:461–473. [PubMed: 18458156]

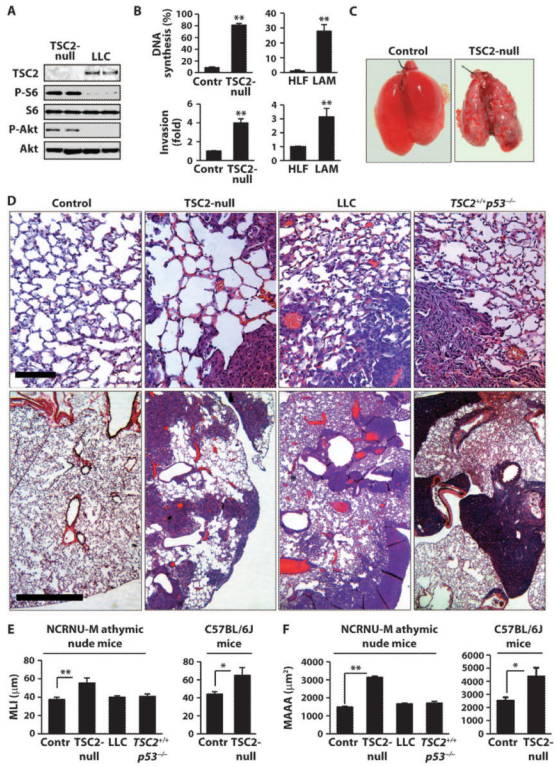

Fig. 1.

TSC2-null lung lesions induce alveolar destruction. (**A**) Immunoblot analysis of TSC2-null and TSC2-positive LLC cells with specific antibodies to detect indicated proteins. (**B**) DNA synthesis and invasion of TSC2-null, control epithelial NMuMG (Contr), human LAM cells, and control human lung fibroblasts (HLF). Data are means ± SE from three independent measurements. $^{**}P < 0.001$ for Contr versus TSC2-null and HLF versus LAM by analysis of variance (ANOVA) (Bonferroni-Dunn). (**C**) Lungs of vehicle-injected (Control) and TSC2-null cell–injected female NCr athymic nude (NCRNU-M) mice at day 15 after injection. (**D**) H&E analysis of lungs at day 15 after tail vein injection of vehicle (Control) or TSC2-null, LLC, or $TSC2^{+/+}p53^{-/-}$ cells. Scale bars, 100 μm (top) and 1000 μm (bottom). (**E** and **F**) Analysis of MLI (E) and MAAA (F) of lungs from NCRNU-M and C57BL/6J mice at day 15 after injection of vehicle (Contr) or TSC2-null, LLC, or $TSC2^{+/+}p53^{-/-}$ cells. Data are means ± SE of $n > 8$ in each group by ANOVA (Bonferroni-Dunn). $^{**}P < 0.001$ for Contr versus TSC2-null cell–injected NCRNU-M mice; $^{*}P < 0.05$ for Contr versus TSC2-null cell–injected C57BL/6J mice.

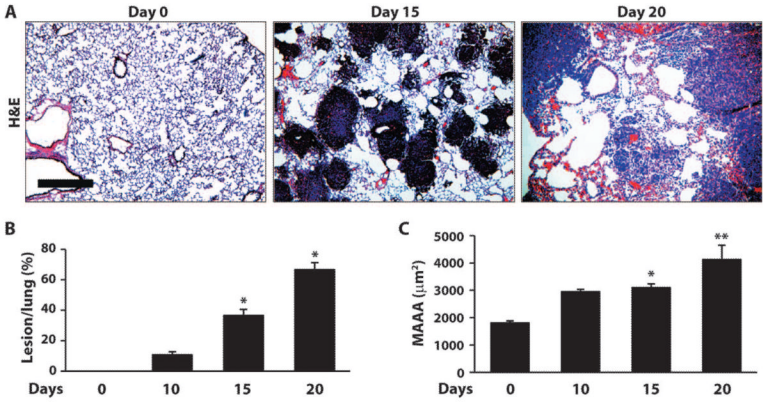

Fig. 2.

Time-dependent alveolar airspace enlargement is associated with TSC2-null lesion growth in the lung. (**A**) Representative images of H&E-stained lungs collected at days 0, 10, 15, and 20 after injection. Scale bar, 200 μm. (**B** and **C**) Lesion/lung ratio and MAAA, calculated with Image-Pro Plus program. (B) Data are means (percentage of the lesion area to the total lung area) ± SE of $n = 8$ in each group. *$P < 0.01$ for day 15 versus day 0; **$P < 0.001$ for day 20 versus day 0 by Fisher. (C) Data are means ± SE of $n > 5$ in each group. *$P < 0.01$ for day 15 versus day 0; **$P < 0.001$ for day 20 versus day 0 by Fisher.

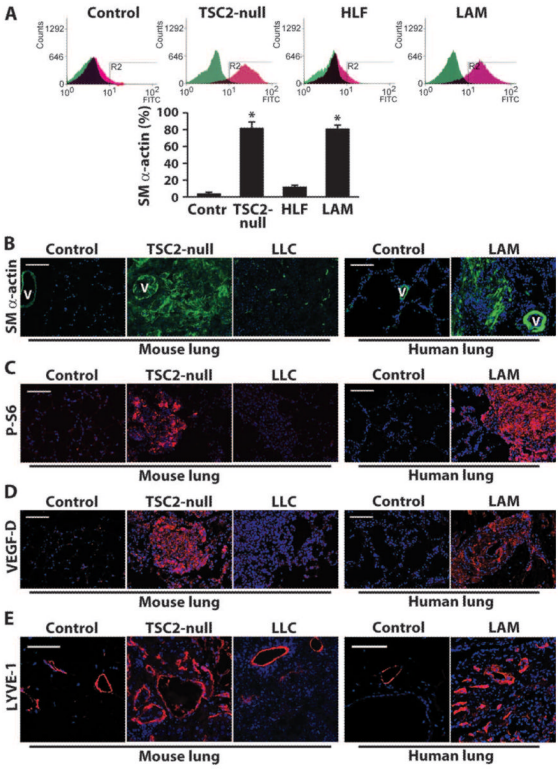

Fig. 3.

SM α-actin–positive TSC2-null lesions show mTORC1 activation, increased VEGF-D, and lymphangiogenesis. (**A**) Fluorescence-activated cell sorting (FACS) analysis of epithelial NMuMG cells (Control), TSC2-null cells, control HLF cells, and human LAM cells with fluorescein isothiocyanate–conjugated SM α-actin antibody (purple) and control immunoglobulin G (green). Data are means ± SE from three independent experiments. **P* < 0.001 for Control versus TSC2-null and HLF versus LAM by ANOVA (Bonferroni-Dunn). (**B** to **E**) Lung tissue sections stained for SM α-actin (B), P-S6 (C), VEGF-D (D), and LYVE-1 (E). Mouse lung specimens (Control, TSC2-null, and LLC) collected at day 20 after vehicle, TSC2-null, or LLC cell injection, and control and LAM human lung specimens were subjected to immunohistochemical analysis with anti–SM α-actin (green), anti–P-S6 (red), anti–VEGF-D (red), and anti–LYVE-1 (red) antibodies. 4',6-Diamidino-2-phenylindole staining (blue) indicates nuclei. Representative images were taken with a Nikon Eclipse TE-2000E microscope. V, vessel. Scale bars, 100 μm.

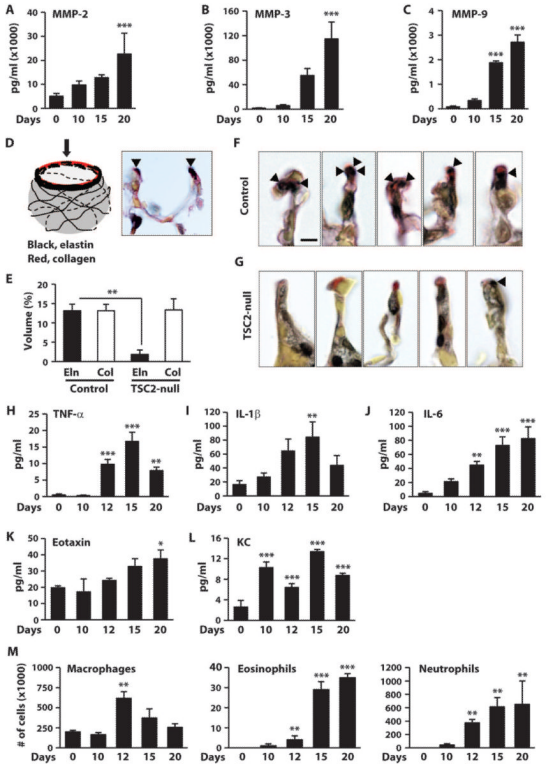

Fig. 4.

Increases in MMPs, inflammatory cells, and cytokines and decrease in alveolar elastin are associated with TSC2-null lung lesion growth. (**A** to **C**) MMP expression assessed in the cell-free supernatant of the BAL fluid at the indicated time points. A multiplex assay was performed by Searchlight technology (Aushon Biosystems). Data are means ± SE of $n = 11$ in each group. ***$P < 0.001$ for days 15 and 20 versus day 0 by ANOVA (Bonferroni-Dunn). (**D**) Schematic representation of elastin and collagen disposition in the alveolar neck. (**E**) Volumes of elastin (Eln) and collagen (Col) in alveoli of Control and TSC2-null lesion–carrying mice. Elastin and collagen were analyzed in alveoli necks of vehicle-injected (Contr) and TSC2-null cell–injected (TSC2-null) mice and expressed as percentage of the total volume of the alveolar neck. Data are means ± SE. **$P < 0.01$ for Control versus TSC2-null lesion–carrying mice by ANOVA (Bonferroni-Dunn). (**F** and **G**) Representative images of alveoli necks of vehicle-injected (Control) (F) and TSC2-null cell–injected (TSC2-null) (G) mice. Verhoeff's elastin stain and Picro-Ponceau counterstain were used to detect elastin (black) and collagen (red), respectively. Arrowheads, elastin-enriched areas. Scale bar, 10 μm. (**H** to **L**) Proinflammatory cytokine and chemokine expression assessed with a multiplex assay in the cell-free supernatant of BAL fluid from mice at the indicated time points after tumor inoculation. (**M**) Inflammatory cell counts assessed from the BAL collected at times as indicated after tumor cell inoculation. Data are means ± SE of $n = 11$ in each group. *$P < 0.05$; **$P < 0.01$; ***$P < 0.001$ versus day 0 by ANOVA (Bonferroni-Dunn).

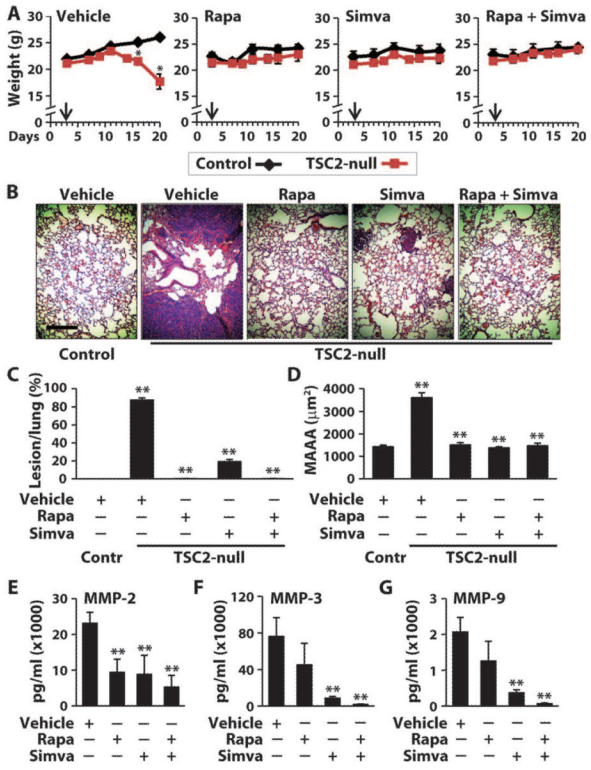

Fig. 5.

Rapamycin plus simvastatin rescues animal survival, prevents lesion growth and lung destruction, and abrogates MMP induction. Mice injected with diluent (Control) or TSC2-null cells were treated with vehicle, rapamycin (Rapa), simvastatin (Simva), and rapamycin + simvastatin (Rapa + Simva) from day 3 after injection. (**A**) Weight of control (black) and TSC2-null cell–injected (red) mice were examined from day 3 (arrows) to day 20 of experiment. Data are means ± SE of $n > 5$ in each group. *$P < 0.01$ for Control versus TSC2-null cell–injected mice by ANOVA (Bonferroni-Dunn). Arrows, beginning of treatment. (**B** to **D**) H&E staining of murine lungs. Scale bar, 500 μm. (B) Lesion/lung ratio (C) and MAAA analysis (D) were performed at day 20 after injection. Data are means ± SE of $n > 8$ in each group. **$P < 0.001$ for Control versus TSC2-null cell–injected vehicle-treated mice and for Rapa, Simva, and Rapa + Simva versus vehicle for TSC2-null cell–injected mice by ANOVA (Bonferroni-Dunn). (**E** to **G**) Expression of MMP-2 (E), MMP-3 (F), and MMP-9 (G), assessed in the cell-free supernatant of BAL at day 20 by multiplex assay. Data are means ± SE of $n > 6$ in each group. **$P < 0.001$ for compound- versus vehicle-treated mice by ANOVA (Bonferroni-Dunn).

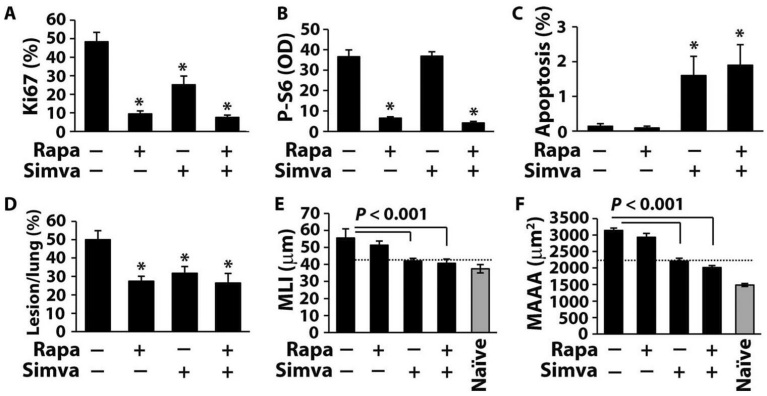

Fig. 6.

Rapamycin and simvastatin differentially affect TSC2-null lesion growth and airspace enlargement. Mice, injected with TSC2-null cells, were treated with vehicle (−), rapamycin (Rapa), simvastatin (Simva), and rapamycin + simvastatin (Rapa + Simva) from day 10 after injection of TSC2-null cells. (**A** to **D**) Effects of drug treatment on lesion growth and airspace enlargement. (A) DNA synthesis (a percentage of Ki67-positive cells per total number of cells), (B) P-S6 [optical density (OD)], (C) apoptosis [a percentage of terminal deoxynucleotidyl transferase–mediated deoxyuridine triphosphate nick end labeling (TUNEL)–positive cells per total number of cells], and (D) percentage of lesion tissue per total lung area at day 20 after injection. Data are means ± SE of $n > 10$ in each group. *$P <$ 0.001 for compound- versus vehicle-treated animals by ANOVA (Bonferroni-Dunn). (**E** and **F**) MLI (E) and MAAA (F) analyses of lung tissue sections collected at day 20 after injection. Data are means ± SE of $n > 8$ in each group by ANOVA (Bonferroni-Dunn). Gray bars, naïve (non-injected vehicle-treated) animals.